A Micromolding-based Evaporation-Polymerization Technique for Rapid and Tunable Fabrication of Hydrogel Films Containing Micropatterned Opal Structures

A thesis submitted by

Maurice Bukenya

In partial fulfillment of the requirements

for the degree of

Master of Science in Chemical Engineering

TUFTS UNIVERSITY

August 2018

Thesis Committee Members:

Advisor and Chair: Dr. Hyunmin Yi

Dr. Ayse Asatekin

Dr. Qiaobing Xu

Abstract

Opal-structured thin-film hydrogel materials hold great potential for utility in a wide range of sensing applications. However, it remains significantly challenging to synthesize these films in a rapid, inexpensive and reliable manner. Prevailing techniques especially suffer from long opal deposition times, and often tend to involve complex and relatively expensive steps. In this thesis, I examined a reliable, rapid and inexpensive micromolding-based evaporation-polymerization method for fabricating poly (ethylene glycol)-based opal-structured thin films. Specifically, intense, highly uniform opalescent colors were achieved by filling microwells in a PDMS mold with Polystyrene (PS) bead solution and allowing the liquid in the bead solution to evaporate in a controlled manner so that the PS beads were arranged into a Face-centered cubic (FCC) structure. Then, upon drying, the interstitial spaces of the packed structure were filled with a UV-curable poly(ethylene glycol) diacrylate (PEGDA) prepolymer solution. The prepolymer solution was polymerized under UV light and the opal-containing PEG films recovered by peeling them off from the mold. Opal deposition using my evaporation-aided technique reduces deposition time to 30-45 minutes only. In addition, the as-prepared films show high tunability of opal color by simply changing PEGDA content in the prepolymer solution. Swelling and de-swelling studies show highly reversible and tunable responsiveness of the films to wetness, pointing to potential applications in humidity sensing. Finally, SEM images confirm the preservation of the FCC structure of the opals in these films.

Table of Contents

List of Figures

List of Equations

Introduction

Synthetic hydrogel thin film materials containing three-dimensional opal structures (opal hydrogel films) have attracted a great deal of attention due to their potential for wide-ranging reagentless detection applications in chemical/ biological sensors[1,2] and humidity sensors[3]. Their brilliant display of visible colors and the absence of risks of discoloration could eliminate the need for chemical reagents, which are otherwise needed to track stimuli-triggered responses.[4] Opal Hydrogel materials can also be engineered to be responsive to a variety of stimuli such as temperature, solvents, biomolecules, mechanical stresses, pH, ionic strength, magnetism and electrical fields.[1,5]

Opal hydrogel film fabrication is often a sequential two-step process which involves first depositing nanospheres into crystal lattices, followed by filling interstitial spaces of the lattices with a polymerizable hydrogel precursor solution which is crosslinked to capture the opal structures. There exist many opal deposition methods such as sedimentation, centrifugation and evaporative deposition techniques.[4] Sedimentation is a self-assembly technique in which colloidal sphere particles are allowed to settle naturally under gravity.[6] While this technique is cheap, it is extremely slow, and particles could take anywhere from weeks to months to form well-ordered lattices. For centrifugation, colloidal sphere particles settle rapidly but it is a relatively expensive process and it is restricted to use of centrifuge tubes as substrates for deposition, a major inconvenience.[1,7]

Meanwhile, evaporation-induced deposition has emerged as a promising alternative to sedimentation and centrifugation. It is much more rapid than sedimentation and produces better opal structures.[1] On the other hand, it is cheaper and more convenient to implement

than centrifugation. In this technique, the liquid phase of a colloidal dispersion is allowed to evaporate, causing the colloidal spheres to settle under the influence of capillarity forces.[7] However, a number of evaporative-deposition-based techniques can still take five (5) hours or longer to form well-ordered opal structures.[3] In short summary, there exists a crucial need for a simple and reliable deposition technique to generate artificial opal structures.

Meanwhile, capture of opal structures into more permanent forms such as incorporating them into other functional materials in a reliable and inexpensive manner continues to be a challenge. Reported methods[8] of achieving this tend to involve many relatively complex steps and to take long[3]. Therefore, there is a need for an efficient technique for incorporating opal structures into functional materials such as hydrogels.

To solve the challenges in prevailing techniques, I propose a simple micromolding-based evaporation-polymerization method for depositing and integrating opal structures into PEG hydrogels, as shown in the scheme of **Figure 1a**.

(a) Micromolding-based Fabrication of Micropatterned Opal-structured Hydrogel Films

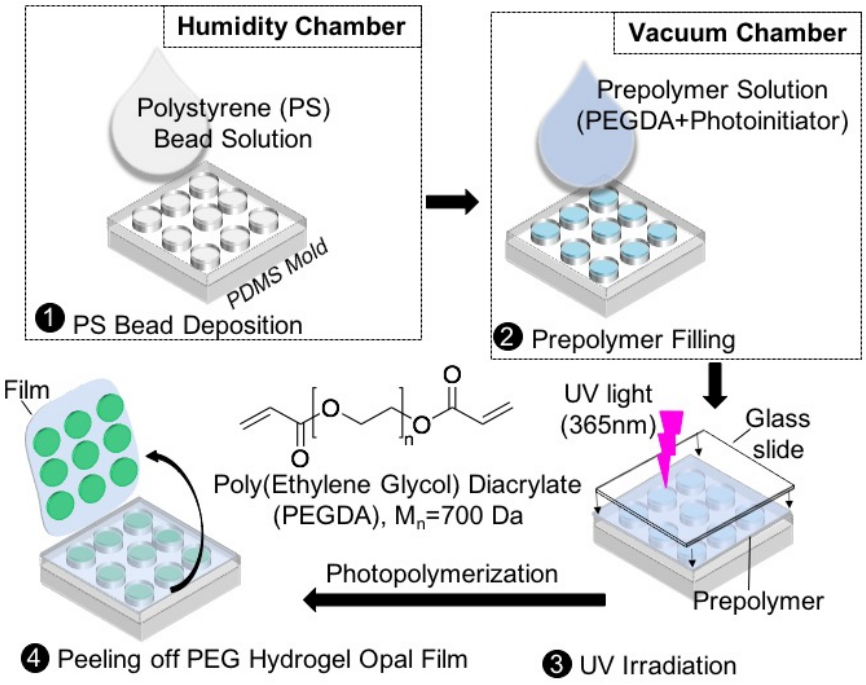

(b) Photograph of Mold After Opal Deposition and (b) Photograph of the Derived Opal Hydrogel Film

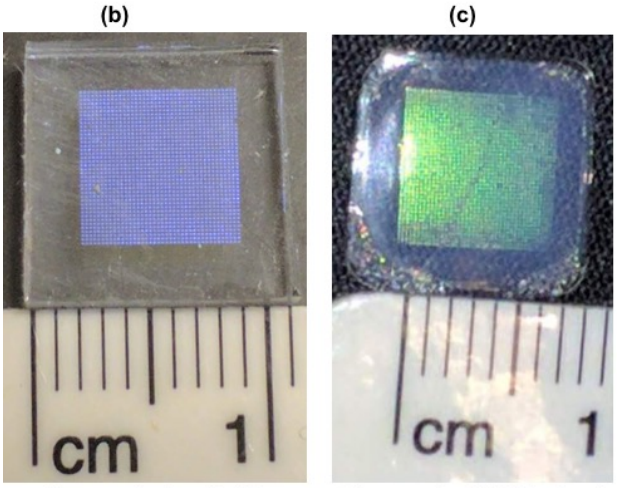

Photograph of mold with deposited PS beads

Photograph of PEG Hydrogel Film

Figure 1. Scheme of micropatterned PEG-based opal-structured Film fabrication and photographs of sample mold and resulting opal film.

(a) Schematic diagram of the fabrication process. (b) Photograph of micropatterned PDMS mold with circular microwells after deposition of Polystyrene (PS) beads. (c) Photograph of Micropatterned PEG hydrogel film containing opal structures.

Briefly, polystyrene beads are packed into crystal lattices (opal structures) by evaporation-aided deposition in microwells of a patterned PDMS mold. Next, the interstitial spaces of the packed PS beads are filled with a photocurable prepolymer solution by vacuuming. This precursor solution is polymerized by exposure to ultraviolet light with a simple handheld UV lamp to capture and hold the PS beads in place. The polymerized film containing the incorporated opal structures is then gently peeled off from the mold. **Figure 1 b** shows a photograph of a mold containing opal structures displaying a uniform purple color, while **Figure 1c** shows a photograph of the derived micropatterned opal-structured hydrogel thin film (area: $1cm^2$) which displays a highly uniform green color.

In this thesis, I examined several critical parameters for reliable, rapid, tunable and simple fabrication of hydrogel film materials containing optically active micropatterned opal structures. First, I showed that my evaporative deposition technique is simple, robust and rapid, and that it results in highly uniform face-centered cubic (FCC) opaline structures. Second, I demonstrated the reliability of my photopolymerization method and the tunability of opal colors of PEG-based micropatterned hydrogels. Third, I reported on the highly reversible and tunable responsiveness of these films to wetness and showed that this responsiveness makes them good candidates for humidity sensing.

Finally, I used scanning electron microscope (SEM) results to show that polystyrene spheres (PS beads) pack into an FCC structure and that the structure is preserved when the particles are incorporated into the PEG hydrogel.

Combined, these results indicate a reliable and tunable fabrication method to produce promising functional materials. I envision that the methodologies presented in this work can be readily extended to include other functional copolymers for a variety of additional properties and applications.

Backgrounds

Structural Color

Opals belong to a class of materials referred to as photonic Crystals (PhCs)[9]. Photonic materials consist of spheres of sizes that fall within the wavelength range of visible light, in a matrix of other material(s) different from the material of the spheres. Spheres are arranged in a periodic pattern to form a lattice structure. The refractive index contrast arising from the composite nature of these materials and the periodic arrangement of the spheres gives rise to a photonic bandgap (PBG), which prevents propagation of light of specific wavelengths through the material. This light is diffracted back out of the material and it emerges as a colored light. Photonic materials do not contain color pigments, but they give off color simply due to diffraction of white light caused by the periodicity of the composite lattice. Thus, opal color is also known as structural color.

Natural and Artificial Opals

In nature, structural color has been reported in a wide range of substances and animals. For example, gemstones contain highly ordered and closely packed silica spheres, which are responsible for their display of color. Wings of some species of butterflies such as *Morpho Didus* and feathers of some birds have also been found to contain structural colors.[7]

By mimicking structures of natural opals, artificial opals can be synthesized by assembly of appropriately sized spheres into well-ordered crystal structures. Common types of materials for such spheres include polymers[10] such as polystyrene and PMMA, and inorganic materials such as silica[11].

FCC Structures

There exist many types of crystal structures into which spheres can pack. The most efficient and most closely packed type of structure is called the face-centered cubic (FCC) structure. In an FCC structure consisting of hard spheres, each sphere is in contact with twelve (12) other spheres and the void fraction is 26%.

The Bragg-Snell Law

The color of diffracted light is described by the Bragg-Snell law (**Equation 1**)[9] and it depends on the refractive index contrast and the diffracting plane spacing, d.

$$m\lambda = 2d\sqrt{n_{eff}^2 - \sin^2(\theta)}$$

Equation 1. Bragg-Snell Law[12]

Where m is the order of diffraction, d is the diffracting plane spacing, n_{eff} is the effective composite refractive index and θ the angle of incidence of light with respect to the normal.

For an FCC structure consisting of hard spheres with incident light at 0°, the predicted wavelength modifies to **Equation 2** below.

$$\lambda = \frac{\sqrt{8}}{\sqrt{3}} * d * \sqrt{n_{ps}^2(1-\phi) + n_{void}^2(\phi)}$$

Equation 2. Modified Bragg-Snell Equation for FCC packing[8]

Where $\boldsymbol{\lambda}$ is the wavelength of observed color, d is the diffracting plane spacing, n_{ps} is the refractive index of sphere material, ϕ is the void fraction (0.26 for FCC) and n_{void} the refractive index of the matrix material.

Fabrication of Artificial Opals

Artificial opals can be assembled using a variety of techniques, the most notable ones including sedimentation, centrifugation and evaporative deposition.[1] Sedimentation is among the simplest and oldest the oldest opal deposition techniques. Sphere particles sediment to the bottom of the substrate under the influence of gravity. For nano-sized spheres, this method is highly inefficient as particles may take up to months to settle and to achieve long-range order.

Centrifugation drives particles to pack into ordered lattices several times faster than sedimentation due to the strong centrifugal forces.

Evaporative deposition on the other hand is intermediate between sedimentation and centrifugation in terms of deposition or packing time. It is faster than sedimentation but slower than centrifugation. During evaporative deposition, the sphere particles pack under

the influence of a combination of capillarity and gravity as the liquid phase of the colloidal dispersion evaporates. I used the evaporative deposition technique for this thesis. Synthetic opals already have applications in photovoltaics, metamaterials, optical fibers and many other areas[1]

Polymeric Hydrogels

Meanwhile, incorporating opal structures into polymeric hydrogels enhances their functionality and the broadens the range of possible applications of the resulting opal-structured materials, due to the combined value of opal and hydrogel properties. Hydrogels consist of flexible three-dimensional networks of crosslinked polymer chains.[13] They are capable of holding large volumes of water and biological fluids due to their adjustable meshes and hydrophilicity. Hydrogels can be functionalized[14] to give them the ability to respond to stimuli such as pH, ionic strength, temperature, mechanical stresses and magnetic fields. They absorb and desorb water and other chemical substances and swell or deswell readily in response to appropriate stimuli. Due to these advantages, hydrogels have been used widely in different types of sensors in different areas.[3]

Polymeric hydrogels can be synthesized via a variety of ways[14] such as the free radical chain photopolymerization reactions, Michael type addition reactions and Schiff base formation reactions.[15] I employed the free radical chain photopolymerization reaction for this thesis, which is simple, rapid and can be carried out at room temperature. The mechanism of this reaction involves 3 steps, namely; initiation, propagation and termination. Initiation involves formation of two free radicals from the dissociation of the initiator molecule. Propagation follows next with the combination of the free radical and the monomer to induce chain elongation. The growth of the chain stops at the termination

step. In this thesis, poly(ethylene glycol) diacrylate (PEGDA, Mn=700Da) was used to make PEG-based hydrogel films with 2-hydroxy-2-methylpropiophenone as the initiator (PI) molecule. PEG is non-toxic, biocompatible and highly flexible making it a good material for safe sensor applications.[8,13]

Micromolding

Lastly, micromolding refers to the technique of replicating microstructures into polymers using molds.[16] In this thesis, I utilized micromolding to incorporate opal structures into PEG hydrogels using a polydimethylsiloxane (PDMS) Mold with patterned microwells as follows: First, I scratched a polystyrene (PS) bead suspension into the microwells of the PDMS molds, allowed the solution to evaporate and the PS beads to form opal structures. Next, I filled the interstitial spaces of the opals with the prepoplymer solution and then polymerized the solution. Finally, I recovered the polymer with its opal structures by peeling it off from the mold. Compared to other techniques such as contact lithography and flow lithography, micromolding allows for simple, reliable and inexpensive replication of complex microstructures into polymers.

Materials and Methods

Materials

Monodisperse polystyrene (PS) beads of varying diameters were fabricated by our collaborator Mr. Jun Hyuk Lee at Professor Piljin Yoo's group of Sungkyunkwan University in Korea. Ethanol (190 proof) was purchased from Decon Laboratories (King of Prussia, PA). Tween 20 (TW20), and Poly(dimethylsiloxane) (PDMS) elastomer kits (Sylgard 184) were purchased from Corning. Poly (ethylene glycol) diacrylate (PEGDA, average Mn 700 Da) and 2-hydroxy-2-methylpropiophenone (Darocur 1173, photoinitiator, PI) were purchased from Sigma-Aldrich (St. Louis, MO). All chemicals were analytical grade and used without further purification. Deionized water was used wherever water was needed.

Equipment

(1) 8W hand-held UV lamp (Spectronics Corp., Westbury, NY). (2) Epifluorescence microscope (Olympus BX51 equipped with a DP70 microscope digital camera, Center Valley, PA). (3) 108 Auto Sputter Coater from Ted Pella, Inc., Redding, CA. (4) JEOL 5910 Scanning Electron Microscope (SEM). (5) USB2000-FL UV-vis spectrometer from Ocean Optics attached to an ''R'' reflectance sensor probe, all connected to a laptop with SpectraSuite Software.

Making PDMS Molds

To fabricate the molds, Sylgard elastomer was mixed with 10% (w/w) curing agent. The mixture was poured onto a silicon wafer containing circle-shaped well patterns in a dish. The mixture was degassed in a vacuum chamber and then thermocured at 65ºC

overnight. The crosslinked PDMS was cut out of the petri dish to recover PDMS molds containing 40x40 circle-shaped micromolds (microwells).

Deposition of PS beads into Opal Structures

Step 1 in the scheme of **Figure 1** illustrates the deposition of PS beads. Polystyrene bead solutions were prepared by diluting PS bead latex suspensions with 190-proof ethanol and Tween20 (~0.1% v/v) in tubes. In a humidity chamber (>93% relative humidity), the solutions were filled into the microwells in PDMS molds by scratching the liquid on the patterned surfaces with pipette tips. The excess PS bead solutions were removed from the molds by pipetting. The molds were left in the humidity chamber for 30 - 45 mins in order for the liquid in the microwells to dry slowly. Upon drying, the beads packed into crystal lattices which were then imaged by darkfield microscopy.

Fabrication of PEG-based Micropatterned Opal Films

The combined steps 2 through 4 of the scheme of **Figure 1** show the subsequent incorporation of the opal structures made in step 1 into PEG hydrogel to produce a PEG-based opal film. Briefly, Prepolymer solutions were prepared by mixing varying percentages of PEGDA (10%v/v, 20%v/v, 40%v/v and 60%v/v) with 1% (v/v) photoinitiator and deionized water. These were then vortexed for 2 minutes and sonicated for 5 minutes to ensure thorough mixing. The solutions were added to molds containing deposited opal crystal structures and forced to seep into the microwells to fill the interstitial spaces of the packed sphere beads by applying vacuum in a vacuum chamber for 30 minutes. The excess prepolymer solutions on the molds were spread into thin liquid films on the surfaces of the molds by placing microscope glass coverslips onto the liquids. The

desired thicknesses of the films were set by introducing supports of the appropriate height for the coverslip. The molds with the coverslips on them were then exposed to UV light (365nm) using a hand-held UV lamp so as to crosslink the prepolymer solutions and form hydrogels. Upon polymerization, hydrogel thin films containing the opal structures were formed and recovered by carefully peeling them off from the mold. The films were washed in deionized water to remove any residual chemicals such as the non-ploymerized PEGDA solution and Photoinitiator. The films were stored in deionized water in a fridge for long periods of time (up to months).

Determination of Final PEG Content in the Opal Films

To determine the post-polymerization PEG composition, wet mass of the films was determined by weighing them on a scale. The films were then dried to constant mass in an oven at 75ºC. The composition was obtained from the ratios of dry weight to wet weight. Note: The mass of PS beads in the films is negligible.

Characterization of the Opal Films

Darkfield micrographs were obtained with an epifluorescence microscope adjusted to the following settings; Filter number 4 and the 10X objective lens were selected, the up light turned was turned on, the exposure time set to $\frac{1}{7}$ seconds, the scale set to 200μm and the samples placed directly perpendicular to the light such that the angle of incidence of light was 0º.

The reflectance spectra were generated with the UV-vis reflectance spectrometer. First, the reflectance was calibrated using a mirror with the reflectance probe pointing perpendicularly towards the mirror so that the angle of incidence of light was 0º. The

mirror was then replaced with the samples and the reflectance spectra of samples measured.

For SEM imaging, samples were prepared by drying them overnight first. They were then coated with gold-palladium layer using the sputter coater, for 10 seconds. They were imaged using the scanning electron microscope, operating at an accelerating voltage of 5kV, at 19000x magnification.

Results and Discussion

Generation of Highly Uniform Opal Structures by Evaporative Deposition

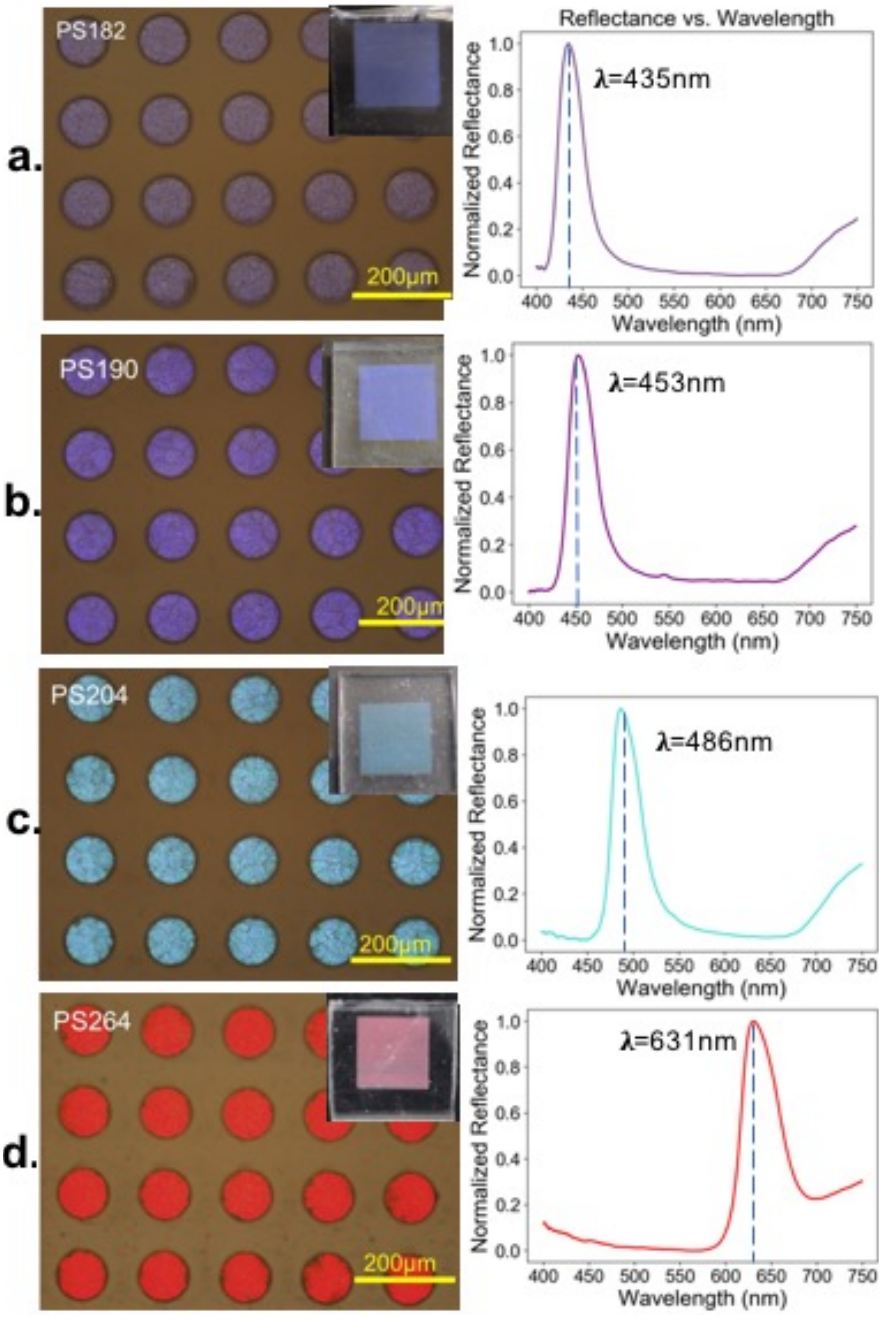

Figure 2. Controlled Deposition of polystyrene (PS) beads into micropatterned Opal structures

(a) - (d) Micrographs and corresponding UV-Vis spectra of opal structures arising from deposition of PS beads of diameters 182nm (PS182), 190nm (PS190), 204nm (PS204) and 264nm (PS264) respectively, in circle-shaped microwells. Insets: Photographs of molds after opal deposition.

As shown in **Figure 2**, I first demonstrate that a micromolding technique can be enlisted to generate micropatterned artificial opal structures via simple evaporative deposition in a controlled and robust manner. For this, I added small volumes of aqueous solution containing polystyrene (PS) beads with varying sizes onto patterned PDMS molds and left the mold in a humidity-controlled chamber to dry slowly. The molds were then imaged with darkfield optical microscopy and the spectra of the molds collected using UV-Vis reflectance spectroscopy (MM).

The micrograph and the inset photograph of **Figure 2a** show that the PS182 beads give faint purple color when deposited into circle-shaped micropatterns, illustrating the formation of "artificial opal" structures via assembly into face-centered cubic (FCC) lattices. Similarly, the micrographs and inset photographs of **Figures 2b, 2c** and **2d** show that PS190, PS204 and PS264 beads deposit into deep purple, turquoise and red colors respectively. All bead types yield highly uniform colors within each pattern and among patterns, illustrating the robust and reliable nature of my simple evaporative deposition method. Note that all four bead types are assembled into opals over a period of only about 30 – 45 minutes, indicating the more rapid nature of this deposition method compared to other methods[3].

Furthermore, the micrographs in **Figure 2** show that the opals are formed in highly regular arrays of circular shapes, rising from the circular-shaped microwells that constitute the pattern of the PDMS mold. Thus, microscale patterning of opal structures can be readily achieved by utilizing patterned molds. Patterning is useful for certain applications.[17] Thus, this method eliminates the need for complex and expensive micropatterning methods or equipment for such applications, further emphasizing the simplicity of my method.

Next, the UV-Vis reflectance spectrum of the opal made with PS182 clearly shows a prominent peak at the wavelength of 435nm, correlating well with the color in the micrograph and the photograph of **Figure 2a.** Similar observations are apparent for PS190 (peak at 453nm), PS204 (peak at 486nm) and PS264 (peak at 631nm) whose peaks also coincide with the colors seen in the micrographs and photographs of **Figures 2b**, **2c** and **2d** respectively. These sharp and prominent reflectance peaks indicate that my simple evaporation method enables reliable and uniform deposition to micropatterned opal arrays yielding brilliant and intense colors.

The results in **Figure 2** show that the evaporation technique employed yields opals with uniform and intense colors that can be readily controlled by the size of PS beads. The uniformity of the colors is indicative of highly ordered packing of the PS beads into face-centered cubic (FCC) structure. On the other hand, the Intensity of the color could be attributed to the uniform deposition coupled with several layers of the deposited PS beads, which generate multiple rays of diffracted light that collectively enhance the brilliance of the observed color.

The UV-reflectance spectra can be utilized to acquire sizes of the PS beads via Bragg-Snell equation. In this thesis work, I employed the modified Bragg-Snell equation, reproduced below, to calculate the PS bead sizes from the spectra peaks.

$$\lambda = \frac{\sqrt{8}}{\sqrt{3}} * d * \sqrt{n_{ps}^2(1-\phi) + n_{void}^2(\phi)}$$

Equation 2. Modified Bragg-Snell Equation for FCC packing

Again, **λ** is the wavelength of color, d is the diffracting plane spacing which in this case is the PS bead diameter, D (i.e., d=D), n_{ps} is the refractive index of polystyrene, ϕ is the void fraction and n_{void} the refractive index of air.

The wavelengths (**λ**) were obtained from the reflectance peaks in **Figure 2**. The refractive indices of PS beads (n_{ps}) and air, which fills the spaces between the PS beads (n_{void}) are 1.59 and 1.0029 respectively. A void fraction ϕ of 0.26 for FCC structures was used assuming the PS beads behaved like hard spheres.

In short summary, the results in **Figure 2** indicate reliable generation of uniform micropatterned opal structures via simple micromolding-based evaporation.

Fabrication of PEG-based Micropatterned Opal Films and Tuning of Opal Color by Varying PS Bead Type and PEGDA Concentration

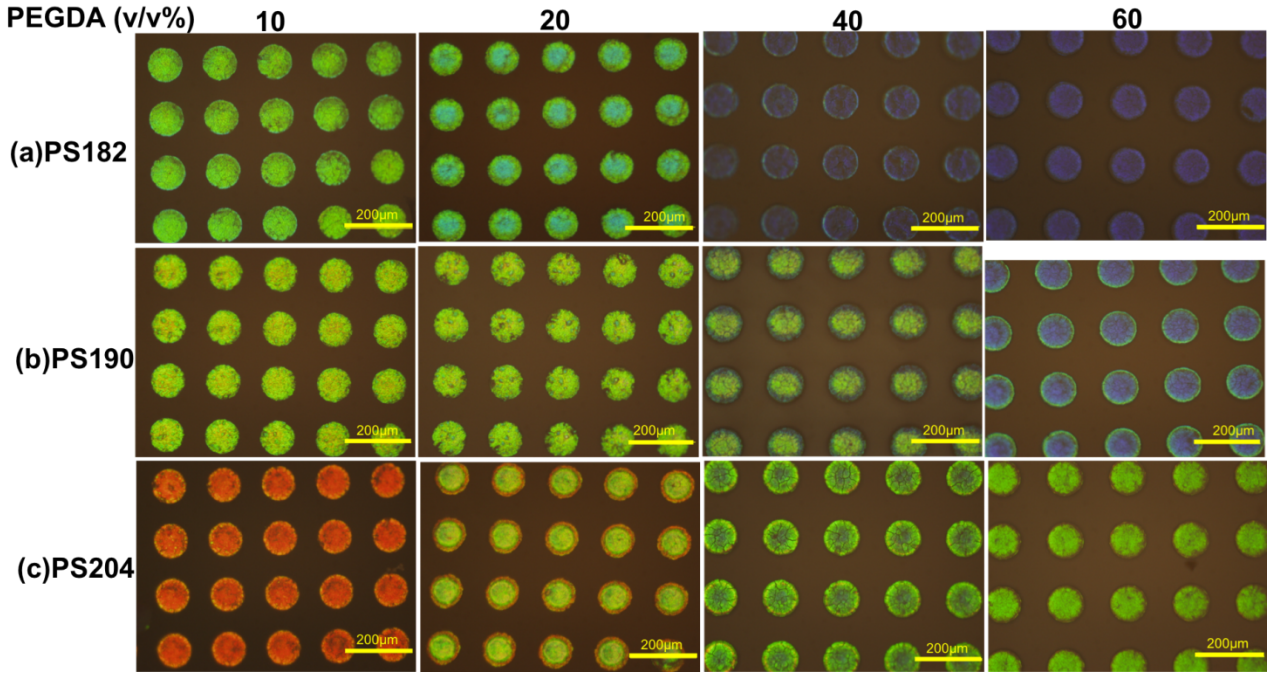

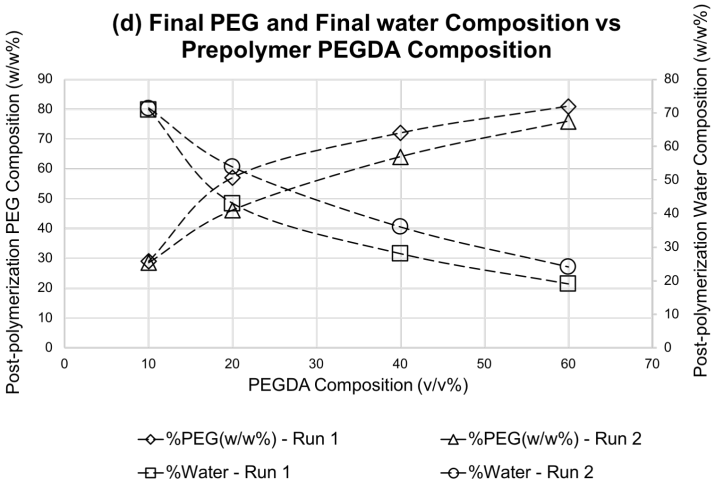

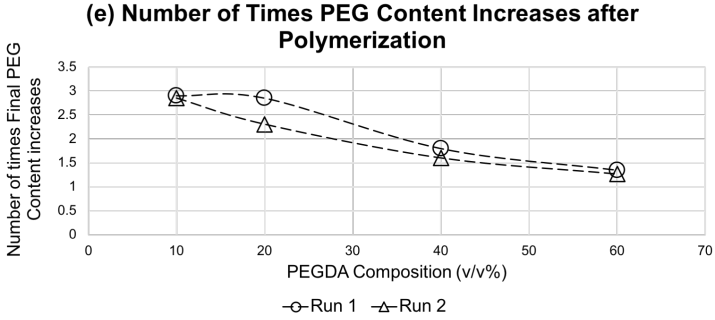

Figure 3. Effects of PEGDA concentration on Opal Color.

Row (a) Darkfield images of four (4) different poly (ethylene glycol) (PEG) hydrogel opal films prepared with PS182 beads and 10%, 20%, 40%, 60% poly(ethylene glycol) diacrylate (PEGDA) (v/v) respectively, immersed in deionized water. Row (b) Darkfield images of PEG opal films prepared with PS190 beads and 10%, 20%, 40%, 60%PEGDA(v/v) respectively, immersed in deionized water. Row (c) Darkfield images of PEG films prepared with PS204 and 10%, 20%, 40%, 60%PEGDA(v/v) respectively, immersed in DI water. (d) Plots of post-polymerization PEG and water composition vs. prepolymer PEGDA composition for two separate sets of films prepared identically with 10%, 20%, 40% and 60% PEGDA. (e) Plots of number of times the Final PEG content is higher than the initial prepolymer PEGDA composition, for the two sets of films reported in **Figure 3d** above.

Next, I demonstrate that opal micropatterns can be incorporated into poly (ethylene glycol) (PEG)-based hydrogel films via a simple photopolymerization method as shown in **Figure 3**. For this, I added aqueous polymerizable solutions containing varying concentrations of PEG diacrylate (PEGDA) and photoinitiator (Darocur 1173) (prepolymer solution) onto the opal micropatterns and exposed them to a handheld UV lamp (365nm) upon covering them with coverslips as shown in the Schematic Diagram of **Figure 1a**. The formed hydrogels were then peeled off from the molds and imaged with darkfield microscopy in deionized water. To determine the actual PEG compositions of the films, I weighed the wet films first, then dried them to constant mass in an oven to obtain the mass of PEG.

The micrographs in **Figure 3** show twelve (12) different opal-containing PEG hydrogel films prepared with varying compositions of PEGDA and PS bead types.

First, row (a) of **Figure 3** shows that the opal structures of hydrogel films prepared with PS182 exhibit green to purple colors depending on the prepolymer PEGDA content. From left to right, the 10%PEGDA opal films display green color, the 20% PEGDA green color with a hint of blue, the 40%PEGDA a bluish-purple color and the 60%PEGDA purple color, illustrating the high tunability of opal color by simply changing the PEGDA content in the prepolymer solution.

Importantly, all the four conditions examined show that the micropatterns were well preserved upon film formation and that the colors remained uniform among and within patterns. This uniformity illustrates the robustness and versatility as well as ready tunability of my simple evaporation-polymerization method.

Likewise, the micrographs in row (b) of **Figure 3** show that the opal structures of the hydrogel films prepared with PS190 give colors ranging from green to blue, depending on the PEGDA content in the prepolymer solution. Specifically, the 10%PEGDA film exhibits a green-yellow color, the 20%PEGDA film opals a green color, the 40%PEGDA film opals a bluish-green color and the 60%PEGDA film opals a blue color. As with the results from PS182, the micropatterns were preserved here and the colors were highly uniform.

Row (c) shows that the opal structures of the hydrogel films of PS204 opals yield orange to green colors. The 10%PEGDA film opals show a red-orange color, the 20%PEGDA film opals a greenish-yellow color, 40%PEGDA film opals a light green color and 60%PEGDA film opals a green color. Again, the micropatterns were well incorporated

into the film and were highly uniform, further supporting the results with PS182 and PS190.

Meanwhile, **Figure 3d** shows the final PEG compositions for two separate, but identically prepared and dried sets of four films prepared with 10%, 20%, 40% and 60% (v/v) PEGDA each. It also shows corresponding compositions of water in the PEG films after polymerization. As can be seen in the plot, final PEG compositions for all films in both sets were higher than the initial PEGDA compositions, indicating an unintended increase PEGDA concentration prior to polymerization. Also, the composition of water in the final PEG film is shown to decrease with increasing PEGDA (and therefore PEG) content, illustrating that high PEG content films have lower water holding capacities than low PEG content films.

Additionally, the plots for the two separate runs yielded significantly different final PEG compositions for the films made with the same PEGDA concentrations, except for the 10% PEDGDA film. This hints at the possibility of existence of uncontrolled experimental variables which cause this phenomenon.

Finally, **Figure 3e** shows a plot of the number of times the final PEG composition was higher than the initial PEGDA composition. The final PEG composition was nearly triple the initial PEGDA composition for the 10% PEGDA films in both sets, over twice the initial PEGDA composition for the 20% PEGDA films, over 1.5 times the initial PEGDA composition for the 40% PEGDA films, and about 1.2 times the initial PEGDA composition for the 60% PEGDA films. The general trend of the decrease in the number of times of increase of PEG composition in the direction of increasing x-axis numbers indicates that

the unintended increase in PEGDA concentration between preparing the prepolymer solution and polymerization is higher in low PEGDA prepolymer solutions than in high PEGDA solutions.

Overall, the results of **Figure 3** show tunability of colors of PEG-based films by simply varying PEGDA content of the prepolymer solution and PS bead type. Firstly, compared to the results of PS182, PS190, PS204 in Figure 2 (Air-PS system), results of the same PS bead types in **Figure 3** (Wet PEG-PS system) appear to be red-shifted at all concentrations of PEGDA reported. This can be attributed to the swelling of the PEG hydrogels which increases the diffracting plane spacing d (i.e., d>D) and results in a larger observed wavelength as according to **Equation 2**.

Secondly, the shifts in color of the opal films in **Figure 3** vary based on PEGDA (or PEG) composition. Specifically, increasing PEG content yields blue-shifts in color, while decreasing PEG content yields red-shifts. I attribute these shifts to two competing factors: the extent of swelling of PEG due to different degrees of crosslinking and differences in refractive indices, the former being the dominant factor.

Low PEG content films swell more than the high PEG content films possibly due to lower polymerization efficiency in the former,[18,13] and therefore lower degree of crosslinking. Specifically, the dense crosslinking of PEG reduces mesh sizes, leaving less room for imbibition of water to induce swelling, while light cross-linking yields larger mesh sizes that facilitate more water uptake and therefore more swelling.[19] Greater swelling leads to larger values of d (d>D) and therefore to larger wavelengths as predicted by the Bragg equation since d and λ are directly proportional. Similarly, less swelling leads to lower

values of d (d>D) and therefore to smaller wavelengths. This explains the red-shifting in the direction of decreasing PEG content and the blue-shifting in the direction of increasing PEG content.

Results of **Figure 3d** provide evidence that refractive index contrast between the wet hydrogel and the PS beads changes with PEG content. Specifically, the change in refractive index contrast is caused by the differences in water content in the PEG hydrogels, which **Figure 3d** shows to decrease with increasing PEG composition. Therefore, refractive index contrast could also be driving these shifts in color.

However, high percentages of water in low PEG content films are expected to lower the overall refractive index of the wet PEG (i.e., the refractive index of the wet PEG system tends towards that of water, 1.33) and thus to cause blue-shifting according to equation 2, which does not appear to be the case for my results. Similarly, the low percentages of water in high PEG content films are expected to increase the refractive index of the wet PEG (i.e., the refractive index is biased towards that of PEG (1.47)) and thus to cause red-shifting according to **Equation 2**. This again is reverse of what my results show. This confirms that the extent of swelling is the more dominant factor in driving the PEG-content color shifts.

Meanwhile, I note that the 60%(v/v) PEGDA film (PS190) and the 20%(v/v) PEGDA film (PS204) appear to have small region around the edges that exhibit different colors than the rest of the opal. For example, the 20%(v/v) opal film in **Figure 3** shows a yellowish-green color overall but the region around the edges is orange. It is not clear why this is the case, but I attribute this occurrence to the different degrees of swelling

between the center and the edges, with the center region being more rigid and swelling less, and the edge being more flexible and swelling more.

Lastly, the results of **Figures 3d** and **3e** show that the post-polymerization PEG composition is always higher than initial prepolymer PEGDA composition. I attribute this to unintended increase in prepolymer PEGDA composition, which could be caused by the evaporation of water from prepolymer solution during vacuuming and UV-irradiation steps. The low pressures achieved during vacuuming and the heat released by the UV lamp during photopolymerization could be aiding and increasing the rate of evaporation of water from the prepolymer solution and causing this phenomenon. **Figure 3e** also seems to suggest that lower PEGDA prepolymer solutions are concentrated several times more than higher PEGDA prepolymer solutions. While it is not apparent why this might be the case, it is possible that the increasing amounts of dissolved PEGDA in the prepolymer solutions slow down the evaporation rate of water. Thus, low PEGDA prepolymer solutions might lose more water to higher evaporation rates and therefore get concentrated more than the high PEGDA prepolymer solutions. Another reason for this could be the low and incomplete polymerization efficiency at low PEGDA compositions.

Due to this phenomenon, and due to the fact that the final PEG compositions may vary even for two identically prepared films (**Figure 3d**), initial PEGDA composition, rather than final PEG content is the reliable parameter to use when reporting results.

Combined, the results of **Figure 3** show reliable and highly tunable synthesis of opal containing hydrogel films by my simple integrated evaporation-polymerization method.

Reversible and Tunable Swelling and Shrinkage of Micropatterned Opal Films

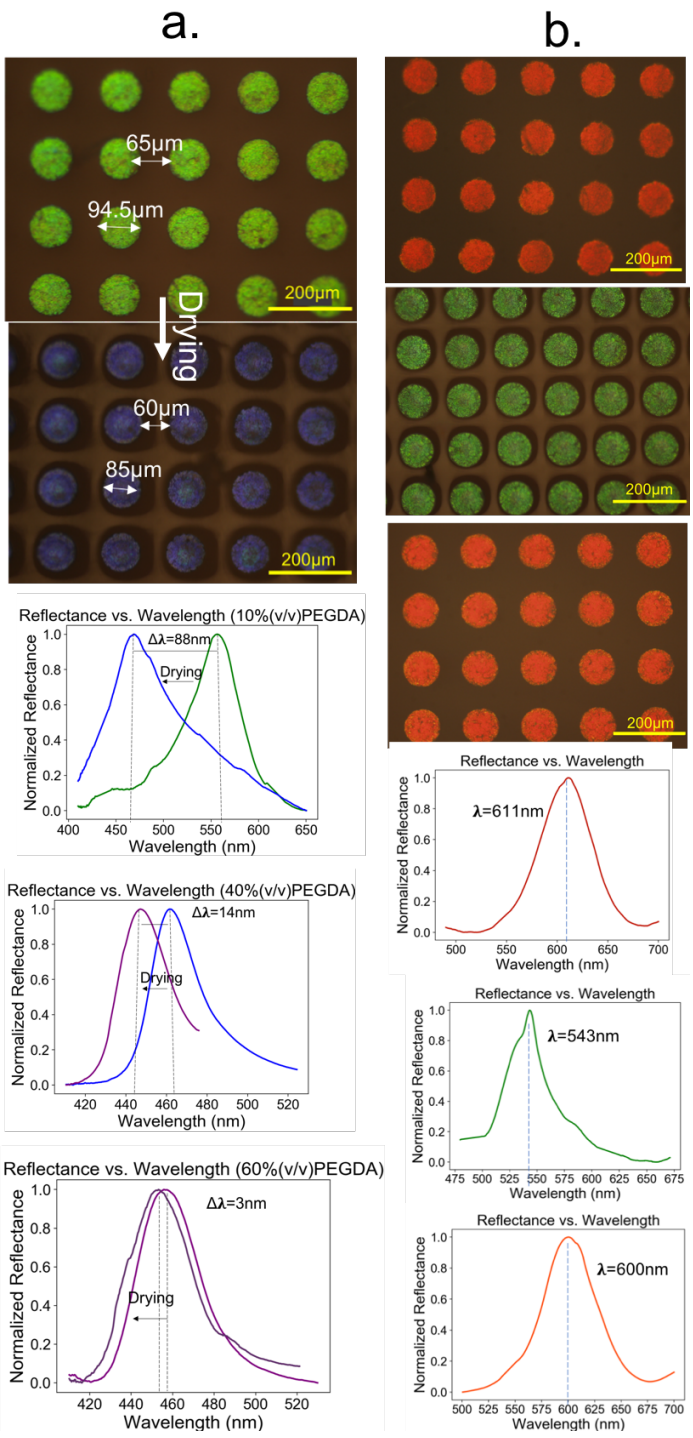

Figure 4. Swelling and shrinkage of opal-structured PEG films due to changes in water content.

Column(a) (Top to bottom): Micrographs showing color change from green to blue of a PS182 10% PEGDA film on drying for 30 minutes in open air at room temperature, and the corresponding UV-Vis reflectance spectrum showing the wavelength shift. The change in wavelength on drying is 88nm. The last two spectra show wavelength shifts resulting from similar drying studies for PS182 films of 40% and 60% PEGDA composition respectively. Column(b) (Top to bottom): Micrographs showing change in color of a PS204 10% PEGDA film from orange to green on drying and a reversal back to orange on rehydrating the film. This reversible process is captured by corresponding changes in wavelengths in the three accompanying UV-Vis spectra.

In **Figure 4**, I show that my micropatterned opal hydrogel films are highly responsive to changes in water content, illustrating a potential utility toward humidity sensing.

For this, I synthesized the films as described previously, dried them in open air at room temperature for 30 minutes and recorded their color and reflectance spectra.

The micrographs of **Figure 4a** show change in color of a PS182 10% PEGDA film from green when the film is immersed in deionized water, to blue when the film is dried in open air at room temperature for 30 minutes. This color change represents a large net change in wavelength of 88nm as shown by the UV-Vis spectrum immediately following the micrographs, indicating the high responsiveness of this film to changes in wetness. The

dramatic and clearly visible color changes make these materials good candidates for optical humidity sensing applications.

The subsequent two spectra of **Figure 4a** show spectra shifts of similar studies but for a PS182 40% PEGDA film and a PS182 60% PEGDA film. Altogether, the three cases show decreasing wavelength shifts with increasing PEGDA concentration from 88nm for the 10% PEGDA film to 14nm for the 40%PEGDA film and finally down to 3nm for the 60% PEGDA one, showing the tunability of the response of our films. These results also indicate that polymer content and degree of crosslinking inversely affect the extent to which the opal film materials respond to wetness, with higher PEGDA composition films showing smaller responses compared to their low PEGDA composition counterparts.

Finally, **Figure 3b** shows three micrographs of the same film (prepared with PS204 and 10%PEGDA) in their initial wet state, the dried state and the rehydrated state respectively. The three reflectance spectra that follow the micrographs each correspond to these three states in their respective order. When dried, the film change from orange to green and when rehydrated it turned back to orange, illustrating the reversibility of the wetting and drying processes. I conducted up to 5 cycles of drying and rehydration on this film (images not shown) and every cycle yielded the same color changes from orange to green and back to orange, another indicator of the robustness our fabrication technique.

PEG-based hydrogels have high affinity for water and can swell readily when supplied with water and shrink as readily when dried.[12,13,8] The change in color of my opal films on drying and wetting is most likely dominated by the change in lattice spacing in the opals due to these events and less by the change in the refractive index contrast as

previously noted. As the PEG film loses water during drying for example, the water-PEG refractive index tends toward the refractive index of PEG (i.e., becomes larger). This is expected to cause a red-shift in the opal color, which clearly is not the case with my drying results in the micrographs of **Figures 4a** and **4b**.

Instead, the lattice parameter plays more apparent role in the color change during the drying and rehydrating processes. Specifically, the micrograph of **Figure 4** shows that the diameters of the opal crystals as measured using ImageJ software decrease from 94.5 microns to 85 microns, a significant net shrinkage of 10%. The inter-opal spacings also show a decrease of 8% upon drying. The decrease in these distances implies a decrease in the lattice spacing, resulting to a decrease in the wavelength of the diffracted light in accordance with **Equation 1**. This explains why all cases of drying (shrinkage of lattice parameters) reported in **Figure 4** resulted in blue-shifting, and the case of rehydration (expansion of lattice parameter to initial state) in **Figure 4c** resulted in red-shifting.

Meanwhile, the inverse relationship between PEGDA content and the wavelength shift upon drying as depicted by the spectra of **Figure 4a** could be attributed to the extent of cross-linking of PEG, where films containing higher amounts of PEG are more heavily cross-linked and are therefore less flexible, while those with lower amounts of PEG are less cross-linked and more flexible, and therefore show larger response to wetness than the latter.

Collectively, the results of **Figure 4** show reversible and tunable response of opal films to humidity and indicate a possible application of these PEG opal films in optical humidity sensors.

SEM Characterization of the Surface and Cross Sections of the Opal Films

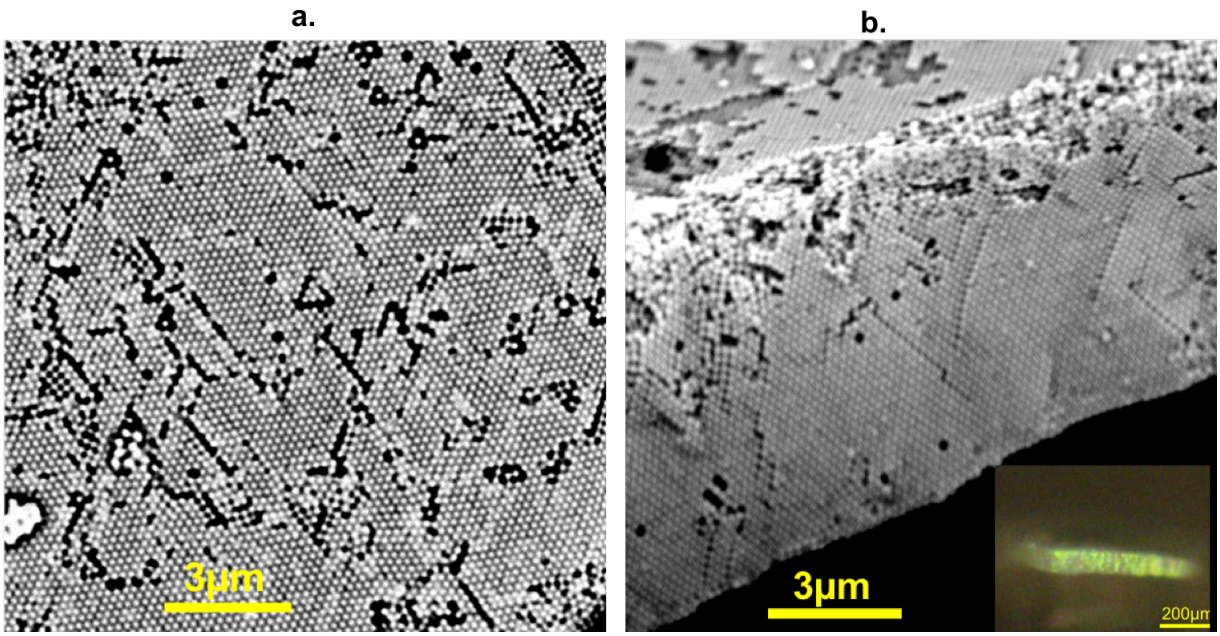

Figure 5. Scanning Electron Microscopy (SEM) Characterization of PEG-opal film made with PS beads of size ~187nm and 20% PEGDA.

(a) SEM Image of the surface. (b) SEM image showing the cross-section through an opal film. The inset is a darkfield micrograph of the cross-section through an opal film.

In **Figure 5**, I demonstrate that the face-centered cubic (FCC) structure of the opals is preserved upon their incorporation into the PEG hydrogel films via my simple polymerization method.

For this, I cut a PEG opal film along the cross-section and imaged it using dark-field microscopy and SEM. I also imaged the surface of the opal of the film by SEM to examine the morphology of both the cross-section and the surface of my films.

Figure 5a shows the surface SEM image of a film made with PS beads of size ~187nm and with 20% PEGDA composition. Despite the many cracks, which are most

likely caused by the excessive drying of the film during preparation for imaging, the FCC ordering of the PS spheres is evident in the surface of the film. This confirms the preservation of the structure of the opal at the surface and further illustrates the robustness of my simple polymerization method.

Meanwhile, **Figure 5b** depicts the SEM image of the cross-section through the film. The inset of **Figure 5b** shows the darkfield micrograph of the cross-section. The SEM image shows highly uniform FCC structure spanning the entire opal thickness from the surface to the bottom. The inset also shows a highly uniform green color that extends through the entire depth of the film, pointing to the highly uniform FCC packing and further supporting the SEM results. Results of **Figure 5b** confirm the presence and preservation of the FCC structure in my films in the layers beneath the surfaces and illustrates the robustness and reliability of prepolymer filling by vacuuming and the subsequent photopolymerization.

The preservation of the FCC structure of the opals when incorporated into PEG films implies that there is little to no disturbance in the opal structure during the vacuuming step as well as the polymerization step, which in turn means that my methods is very reliable and robust.

Combined, results in **Figure 5** show that prepolymer filling via vacuuming and simple photopolymerization by exposure to handheld UV lamp are reliable and robust ways to incorporate the FCC structure of the opals into PEG hydrogels with little or no disturbance of the opal structures.

Conclusion

In this thesis, I demonstrated a simple, rapid and inexpensive integrated evaporation-polymerization technique based on micromolding and its potential application in optical humidity sensors. First, highly uniform artificial opal structures were generated in patterned molds via simple evaporative deposition in a rapid, controlled and robust manner.

Next, I showed that as-generated opal structures can be incorporated into PEG-based hydrogels to produce micropatterned optically active hydrogel films with highly uniform colors that can be tuned simply by changing the prepolymer PEGDA composition. This can be readily and reliably implemented by vacuum-filling the interstitial spaces of the opal structures with photocurable PEGDA solution and then simply exposing the solution to UV light. I then illustrated that the micropatterned hydrogel films are highly responsive to wetness, a property that makes them potential candidates for humidity sensing. Furthermore, this response to wetness is highly tunable and reversible over several drying-rehydration cycles. The response can be tuned simply by adjusting the polymer content of the films. Finally, I used SEM studies to show that the opal structures are well preserved in films, an indicator that the vacuum-filling process and my simple polymerization method do not disturb the particles initially arranged via my evaporative deposition technique.

Overall, my evaporation-deposition technique provides a promising platform for manufacturing highly tunable and responsive opal film materials for a wide range of sensing applications, in a manner that is simple, saves time and that is cheap to implement.

References

1. Armstrong, E.; O'Dwyer, C., Artificial opal photonic crystals and inverse opal structures – fundamentals and applications from optics to energy storage. *Journal of Materials Chemistry C* **2015,** *3* (24), 6109-6143.

2. Zhou, J.; Wang, J.; Huang, Y.; Liu, G.; Wang, L.; Chen, S.; Li, X.; Wang, D.; Song, Y.; Jiang, L., Large-area crack-free single-crystal photonic crystals via combined effects of polymerization-assisted assembly and flexible substrate. *Npg Asia Materials* **2012,** *4*, e21.

3. Yu, B.; Cong, H.; Yang, Z.; Yang, S.; Wang, Y.; Zhai, F.; Wang, Y., Preparation of Humidity-Sensitive Poly(Ethylene Glycol) Inverse Opal Micropatterns Using Colloidal Lithography. *Materials* **2017,** *10* (9), 1035.

4. Lee, H. S.; Kim, J. H.; Lee, J.-S.; Sim, J. Y.; Seo, J. Y.; Oh, Y.-K.; Yang, S.-M.; Kim, S.-H., Magnetoresponsive Discoidal Photonic Crystals Toward Active Color Pigments. *Advanced Materials* **2014,** *26* (33), 5801-5807.

5. Wang, H.; Zhang, K.-Q., Photonic Crystal Structures with Tunable Structure Color as Colorimetric Sensors. *Sensors* **2013,** *13* (4), 4192.

6. Hartsuiker, A.; Vos, W. L., Structural Properties of Opals Grown with Vertical Controlled Drying. *Langmuir* **2008,** *24* (9), 4670-4675.

7. Yeo, S. J.; Choi, G. H.; Yoo, P. J., Multiscale-architectured functional membranes utilizing inverse opal structures. *Journal of Materials Chemistry A* **2017,** *5* (33), 17111-17134.

8. Lee, H. S.; Kubrin, R.; Zierold, R.; Petrov, A. Y.; Nielsch, K.; Schneider, G. A.; Eich, M., Photonic properties of titania inverse opal heterostructures. *Opt. Mater. Express* **2013,** *3* (8), 1007-1019.

9. Gina Mayonado, S. M. M., Valentina Robbiano, Franco Cacialli, Investigation Of The Bragg-Snell Law In Photonic Crystals.

10. Khokhar, A. Z.; Rue, R. M. D. L.; Treble, B. M.; Mccomb, D. W.; Johnson, N. P., Stibnite inverse opal. *IET Micro & Nano Letters* **2008,** *3* (1), 1-6.

11. Miguez, H.; Blanco, A.; Lopez, C.; Meseguer, F.; Yates, H. M.; Pemble, M. E.; Lopez-Tejeira, F.; Garcia-Vidal, F. J.; Sanchez-Dehesa, J., Face centered cubic photonic bandgap materials based on opal-semiconductor composites. *Journal of Lightwave Technology* **1999,** *17* (11), 1975-1981.

12. Son, K.; Lee, J., Synthesis and Characterization of Poly(Ethylene Glycol) Based Thermo-Responsive Hydrogels for Cell Sheet Engineering. *Materials* **2016,** *9* (10), 854.

13. Datta, A., *Characterization of Polyethylene Glycol Hydrogels for Biomedical Applications*. Louisiana State University: 2007.

14. Helgeson, M. E.; Chapin, S. C.; Doyle, P. S., Hydrogel microparticles from lithographic processes: Novel materials for fundamental and applied colloid science. *Current Opinion in Colloid & Interface Science* **2011,** *16* (2), 106-117.

15. Ahmed, E. M., Hydrogel: Preparation, characterization, and applications: A review. *Journal of Advanced Research* **2015,** *6* (2), 105-121.

16. Papautsky, I.; T. K. Peterson, E., *Micromolding*. 2015; p 2102-2116.

17. Ding, T.; Zhao, Q.; Smoukov, S. K.; Baumberg, J. J., Selectively Patterning Polymer Opal Films via Microimprint Lithography. *Advanced Optical Materials* **2014,** *2* (11), 1098-1104.

18. Pregibon, D. C.; Doyle, P. S., Optimization of Encoded Hydrogel Particles for Nucleic Acid Quantification. *Analytical Chemistry* **2009,** *81* (12), 4873-4881.

19. Lin, C.-C.; Metters, A. T., Hydrogels in controlled release formulations: Network design and mathematical modeling. *Advanced Drug Delivery Reviews* **2006,** *58* (12), 1379-1408.